BALLOON MEASUREMENT OF ELECTRIC FIELDS NEAR THE HARANG DISCONTINUITY

Toshio OGAWA,

Geophysical Institute, Kyoto University, Sakyo-ku, Kyoto 606

Hisao YAMAGISHI, Hiroshi FUKUNISHI and Takayuki ONO

National Institute of Polar Research, 9–10, Kaga 1-chome, Itabashi-ku, Tokyo 173

Abstract: Electric fields were measured with three pairs of conducting plate antennas on board a balloon which was launched from Stamsund ($L=6.0$), Norway at 1909 UT on March 20, 1982. During the balloon flight at the ceiling altitude of 32 km, two sequential substorms occurred. The direction of horizontal electric field change can be explained as an electric field behavior near the Harang discontinuity, a boundary between the eastward and westward auroral electrojet currents.

The vertical electric field and current increased greatly when the balloon transversed over the mountainous area. This increase can be interpreted by a mountain effect on the stratospheric electric field. The conductivity obtained by the combination of the vertical electric field and current is estimated $(1\text{–}2)\times 10^{-11}$ S/m and it reconfirms the value of conductivity in the polar stratosphere.

1. Introduction

The balloon experiments have been performed as a cooperative work with the Royal Norwegian Council for Scientific and Industrial Research, Space Activity Division to make a comprehensive study of stratospheric aeronomy associated with auroral activity in the Scandinavian Peninsula. The experimental items were natural VLF waves, omega VLF signals, power line radiations, X-rays (20–100 keV) and static electric fields. In the present paper we give results of the last item.

In the Scandinavian Peninsula ground-based networks of all-sky cameras, riometers, and magnetometers are working and the STARE radars (Scandinavian Twin Auroral Radar Experiment) can monitor the ionospheric electric field. Since unfortunately only one STARE radar worked on the day of the balloon experiment, no comparison could be made with each other.

2. Instrumentation

The dimensions of the payload gondola are $74(\mathrm{W})\times 74(\mathrm{W})\times 65(\mathrm{H})$ cm. The three pairs of antenna plates with the same areas as the sides of the gondola are placed 20 cm apart from each side by using insulating rods. The effective separation of a pair of antenna plates is estimated as 1.14 and 1.05 m for horizontal (X, Y) and vertical (Z) components respectively. The payload gondola contains electronic circuits and

power batteries. The antenna plates and the payload gondola are coated with aquadag to prevent disturbances caused by photoemissions. The resistors of $1\times10^{12}\,\Omega$ are used for the input resistance of the electrometer. The vertical current was measured by switching the input resistors of $1\times10^{12}\,\Omega$ with $5\times10^{9}\,\Omega$ every two minutes (OGAWA, 1973). The intensity range of the electric field detected by this equipment is within 100 mV/m and 1 V/m for the horizontal and vertical components respectively.

The payload gondola was hung about 100 m down from the balloon by drawing out a nylon rope stored in a special reel. Then, it was rotated with 1.5 revolutions per minute by a spin motor. The antenna direction was determined by means of a Hall current sensor placed inside the payload gondola.

3. Observation

A balloon with volume of 15000 m^3 (B_{15}-1N) was launched at Stamsund (68°08′N, 13°50′E; $L=6.0$) at 1909 UT on March 20, 1982, and then it drifted toward the ESE direction. The balloon reached the ceiling altitude of 32 km at 2040 UT. The balloon was cut down at 2255 UT and landed near Rovaniemi in Finland at 2335 UT. During the flight time at the ceiling altitude two substorms occurred, and associated electric field variations were observed.

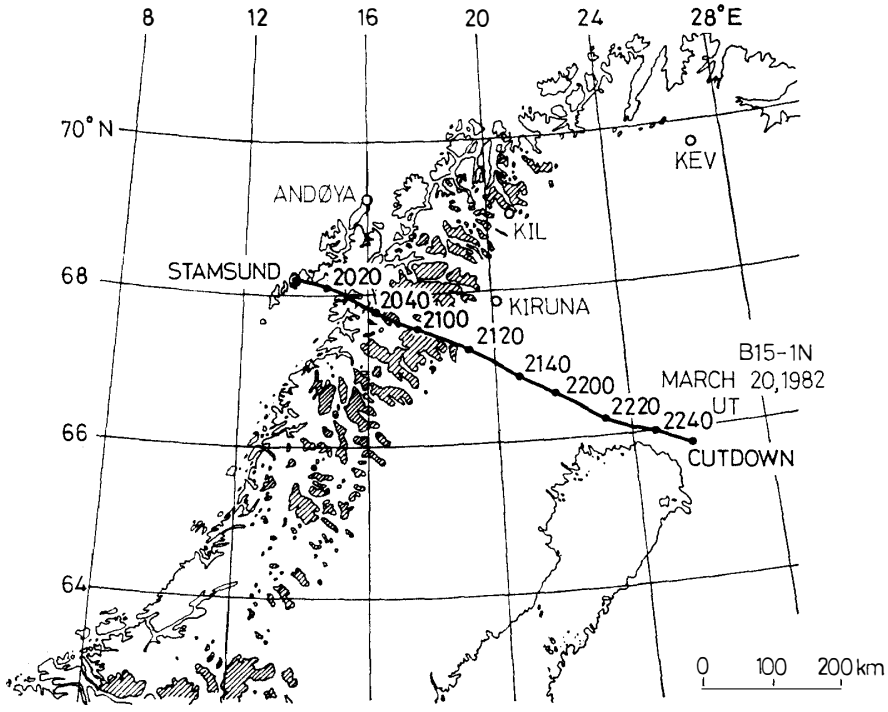

Fig. 1. Balloon horizontal trajectory plotted on the Scandinavian topographical map. The hatched region denotes the mountainous area higher than 1 km above msl.

Figure 1 shows the balloon horizontal trajectory on the topographical map in which mountainous areas higher than 1000 m are indicated by hatch. It shows that the balloon moved transversally over the mountainous area from 2020 to 2120 UT.

4. Observation Results

The temporal variations of the vertical electric field and current obtained by a pair of the vertical antennas are given in Fig. 2. Both the electric field and current had maxima at 460 mV/m and 3.5×10^{-12} A/m^2 respectively before the balloon reached

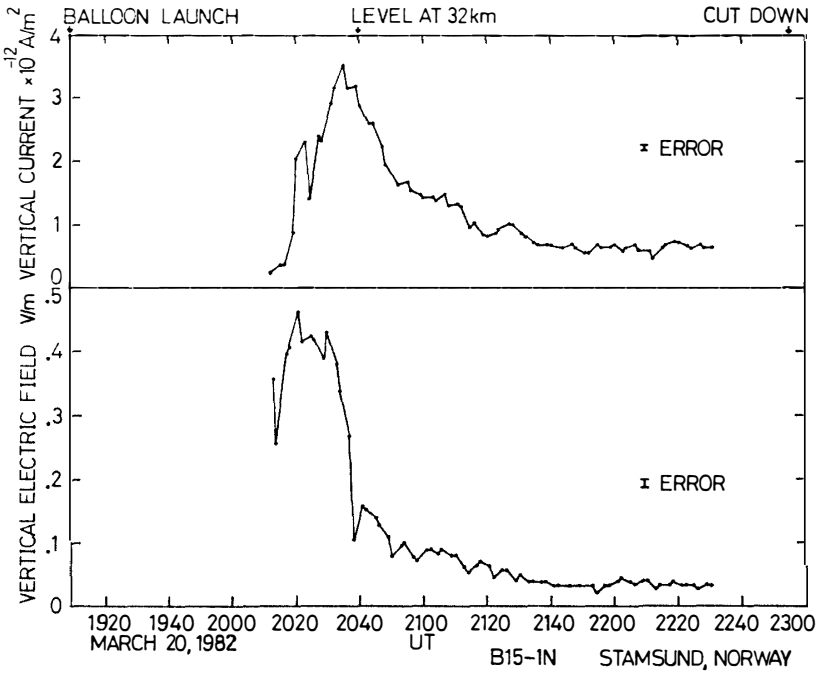

Fig. 2. Observed vertical electric field (lower panel) and vertical current (upper panel).

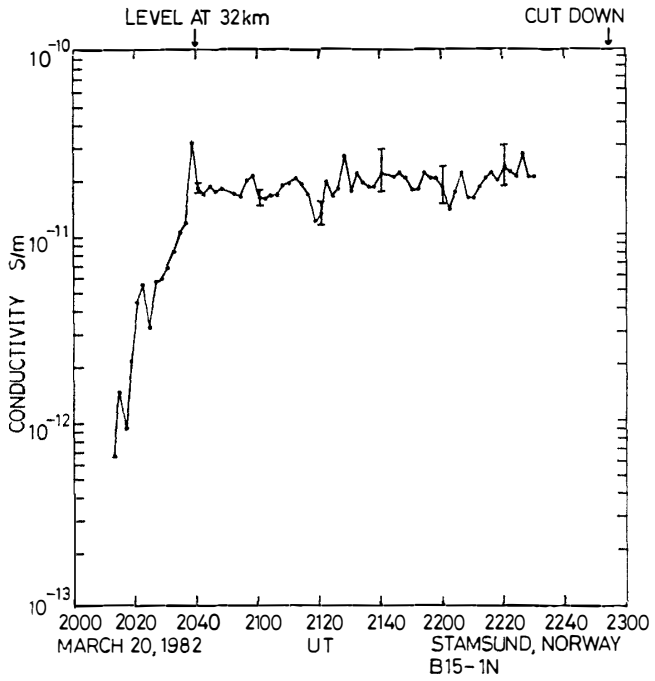

Fig. 3. Electric conductivity derived by taking ratios of vertical current to vertical electric field.

the ceiling altitude of 32 km at 2040 UT. These intensities continued to decrease during the level flight and attained to 40 mV/m and 0.6×10^{-12} A/m^2 respectively.

The atmospheric electric conductivity was estimated by taking ratios of electric current to electric field. The conductivity variation during the balloon flight is given in Fig. 3. The conductivity increased with an increase of altitude until the balloon reached the ceiling altitude. During the balloon level flight the conductivity fluctuated by about 10% from 1.8×10^{-11} to 2.0×10^{-11} S/m.

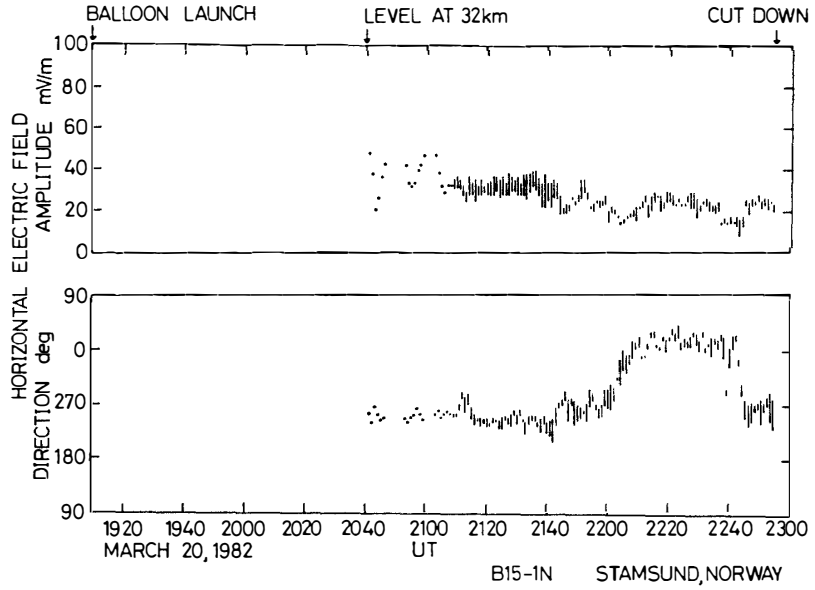

Fig. 4. Variation of horizontal electric field observed on the balloon. The upper panel shows the amplitude, while the lower panel shows the direction.

The observed horizontal electric fields are plotted in Fig. 4. The vertical lines in the figure give the ranges of electric field intensities detected by the two pairs of horizontal (X, Y) antennas. The intensities of electric fields detected by the X and Y antennas should coincide with each other since these antennas were rotating by a spin motor. Therefore, the vertical lines will give a measure of accuracy. The electric field amplitude and direction are shown in the upper and lower panels respectively. The amplitude varied from 30 to 20 mV/m and the direction changed from the west-southwest to the north and then changed to the west.

5. Conclusion and Discussion

5.1. The vertical electric field and current

The vertical electric field and current greatly increased before the balloon reached the ceiling altitude and then decreased during the ceiling. Since electric field data did not have enough accuracy before the balloon reached the ceiling altitude, we investigate the characteristics of electric field only after the ceiling. As seen in Fig. 1 the balloon moved transversally over the mountainous area higher than 1000 m until about 2120 UT and the magnitudes of the vertical electric field and the current are much larger before 2120 UT than that after 2120 UT. Since this increase region of the verti-

cal electric field well coincides with the mountainous region, the great increase before 2120 UT is inferred to be due to the mountain effect as previously pointed by OGAWA and TANAKA (1976). The atmospheric electric field and current are generally produced by the thunderstorm activity and they have diurnal variation with a maximum value at about 20 UT. The great increase of vertical electric field and current before the ceiling is, however, much larger than the variation by the global thunderstorm.

The mountain effect can be calculated as follows. Let the height distribution of the atmospheric conductivity be the sum of two exponential functions. We assume that the boundary height between the two exponentials is z_0, and the conductivity scale height is H_1 in the lower region and H_2 in the higher region of the atmosphere. If we assume further that the mountain height is the same as the boundary height z_0, then the ratio of the electric current flowing onto the mountains I_m to that flowing into the flat area or the ocean surface I_s is given by

$$\frac{I_m}{I_s}=1+\exp\left(\frac{z_0}{H_1}\right)\times\left[\exp\left(\frac{z_0}{H_2}\right)-\exp\left(\frac{z_0}{H_2}-\frac{z_0}{H_1}\right)\right]. \quad (1)$$

Taking $z_0=2$ km, $H_1=3$ km and $H_2=6$ km, then we get $I_m/I_s=2.3$ which is about the same value as that obtained in the present experiment. Therefore, it is suggested that the great increases of the electric field and current between 2040 and 2120 UT during the balloon level flight might have been caused by the mountain effect.

5.2. *Conductivity*

Considering the results observed in this experiment and at Syowa Station in 1972 (OGAWA *et al.*, 1977), it is concluded that the conductivity at the 32 km altitude is $(1\text{–}2)\times10^{-11}$ S/m in the polar region. The conductivity in the auroral zone stratosphere depends on the auroral activity. The conductivity fluctuation of about 10% observed in the present balloon experiment is probably due to the auroral activity.

5.3. *Horizontal electric field*

It was demonstrated by the previous balloon experiment over the Tohoku area of Honshu Island in Japan that not only the vertical electric field but also the horizontal one is affected by the mountain underneath when a balloon floats at low altitude (OGAWA *et al.*, 1975). The present study also shows a mountainous effect on the horizontal electric field as shown in Fig. 4. The electric field intensity during the interval from 2040 to 2120 UT (over the mountainous area) is larger and more scattered than that after 2120 UT.

After 2120 UT the horizontal electric field shows typical nightside variations and varies with associated magnetic activity. Figure 5 shows the ground magnetic field variations observed at Kiruna. As seen in Fig. 5, the first substorm began at around 21 UT, attaining a maximum at 2140 UT and the recovered. The second substorm occurred at 2220 UT. To compare the electric field with geomagnetic activity in the vicinity of the balloon, the electric field is resolved into the north-south component and the east-west one as plotted in Fig. 6.

As shown in Figs. 5 and 6, the direction of the electric field is southwest during the first expansion phase and it turns northward during the recovery phase. Then it turns west-northwest during the second expansion phase.

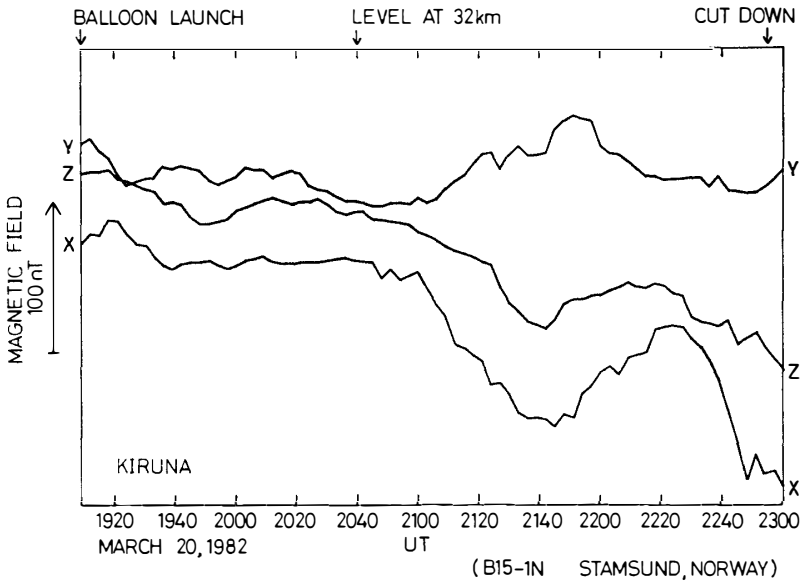

Fig. 5. Magnetic X, Y and Z components observed at Kiruna during the balloon flight.

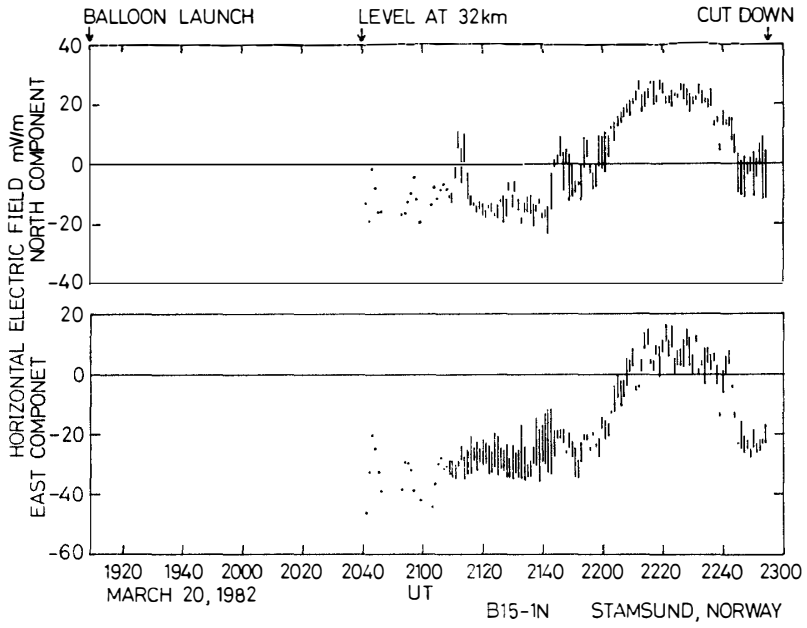

Fig. 6. North component (upper panel) and east component (lower panel) of the observed horizontal electric field.

These electric field variations can be well understood by the movement of the Harang discontinuity region which is inferred from the magnetic field variation at Kiruna. The Harang discontinuity region is defined as the boundary region between a westward electrojet which yields negative magnetic field variation on the ground and an eastward electrojet with positive magnetic variation on the ground. The Harang discontinuity moves depending on the auroral activity. It moves toward lower latitude when the auroral activity becomes high, while it moves toward higher latitude when the auroral activity becomes low. Relationship between the electric field and the

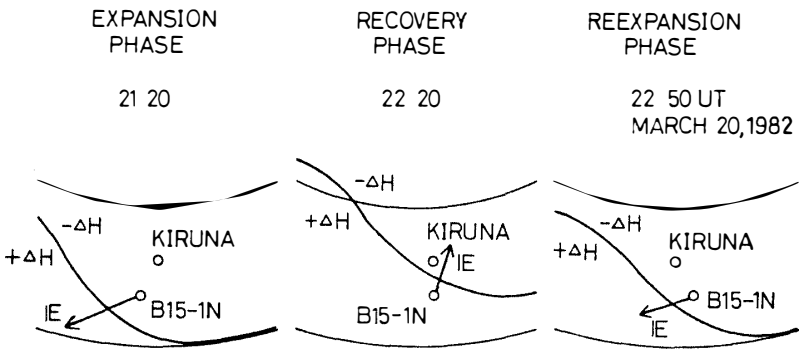

Fig. 7. Behavior of observed horizontal electric fields near the Harang discontinuity during the expansion and recovery phases of the first substorm and the expansion phase of the second one.

Harang discontinuity region is displayed in Fig. 7 for three representative sequential stages; the expansion phase of the first substorm at 2120 UT, the end of the recovery phase of the first substorm at 2220 UT and the expansion phase of the second substorm at 2250 UT. As shown in Fig. 7 it is inferred from the magnetogram at Kiruna that the Harang discontinuity was located at the lower latitude side of the balloon during the expansion phase of the first substorm, and then it moved toward the higher latitude side across the balloon position during the recovery phase. The Harang discontinuity moved again at the lower latitude side of the balloon. This situation would explain the present observation results.

Acknowledgments

We thank B. LANDMARK, A. GUNDERSEN and other staff members of the Royal Norwegian Council for Scientific and Industrial Research, Space Activity Division, and S. ULLALAND of University of Bergen, for their great help in the balloon launching and data telemetry in Norway. We thank J. NISHIMURA and other staff members of the Institute of Space and Astronautical Science for their help in preparing the rotating motor and the letdown reel, and for teaching us the balloon launching technique. We also thank T. NAGATA, director of the National Institute of Polar Research and T. HIRASAWA of the same institute for their appropriate suggestions for the present balloon experiment.

References

OGAWA, T. (1973): Analyses of measurement techniques of electric fields and currents in the atmosphere. Contrib. Geophys. Inst. Kyoto Univ., **13**, 111–137.

OGAWA, T. and TANAKA, Y. (1976): Land effect on the stratospheric vertical electric field and current. J. Atmos. Terr. Phys., **38**, 599–604.

OGAWA, T., YASUHARA, M. and HUZITA, A. (1975): Stratospheric horizontal electric fields over mountains. J. Atmos. Terr. Phys., **37**, 841–844.

OGAWA, T., TANAKA, Y., HUZITA, A. and YASUHARA, M. (1977): Three-dimensional electric fields and currents in the stratosphere. Electrical Processes in Atmospheres, ed. by H. DOLEZALEK and R. REITER. Darmstadt, Steinkopff, 552–556.

(Received February 15, 1984; Revised manuscript received April 5, 1984)